Computational Statistics and Data Analysis 55 (2011) 2819–2829

Contents lists available at ScienceDirect

Computational Statistics and Data Analysis

journal homepage: www.elsevier.com/locate/csda

Adaptive EWMA procedures for monitoring processes subject to linear drifts

Yan Su [a], Lianjie Shu [b,*], Kwok-Leung Tsui [c]

[a] Department of Electromechanical Engineering, University of Macau, Macau

[b] Faculty of Business Administration, University of Macau, Taipa, Macau

[c] School of Industrial and Systems Engineering, Georgia Institute of Technology, Atlanta, GA 30332, United States

ARTICLE INFO

Article history:
Received 22 November 2010
Received in revised form 11 April 2011
Accepted 14 April 2011
Available online 20 April 2011

Keywords:
Average run length
Integral equation
Linear trend
Statistical Process Control
Exponentially weighted moving average

ABSTRACT

The conventional Statistical Process Control (SPC) techniques have been focused mostly on the detection of step changes in process means. However, there are often settings for monitoring linear drifts in process means, e.g., the gradual change due to tool wear or similar causes. The adaptive exponentially weighted moving average (AEWMA) procedures proposed by Yashchin (1995) have received a great deal of attention mainly for estimating and monitoring step mean shifts. This paper analyzes the performance of AEWMA schemes in signaling linear drifts. A numerical procedure based on the integral equation approach is presented for computing the average run length (ARL) of AEWMA charts under linear drifts in the mean. The comparison results favor the AEWMA chart under linear drifts. Some guidelines for designing AEWMA charts for detecting linear drifts are presented.

1. Introduction

Control charts are effective tools in statistical process control (SPC) for process monitoring and quality improvement. The applications of control charts extend far beyond industrial setting toward other areas such as biology, genetics, medicine, and finance (Montgomery, 2009). One of the most important problems in quality engineering is the detection of shifts in process means which occur in different ways. The shift may be a step change in the mean or a drift in the mean in a linear/nonlinear fashion. The step shift stays at the new level since its occurrence while the linear drift gradually increases/decreases over time in the mean. A great deal of attention has been devoted to the monitoring of step mean shifts while relatively less attention has been paid to the monitoring of linear drifts in the mean.

The output characteristics of many manufacturing processes exhibit drifts, and the drift in the mean can be positive or negative, linear or nonlinear. A typical example of positive drifts is tool wear, which describes the gradual failure of cutting tools due to regular operation. A tool wear-out leads to gradually increasing product dimension. An example of negative drifts includes a continuous clogging of a spray nozzle. In both examples, the output characteristics exhibit a drift instead of a step change in the process mean. As the drift in the process mean can cause significant losses in product quality, it is important to detect the drift as soon as it occurs. In practice, the linear model often serves as a good one for many drifts. For simplicity, this paper will limit discussions on the detection of linear drifts.

The conventional control charts for monitoring step shifts, including the Shewhart, cumulative sum (CUSUM), and exponentially weighted moving average (EWMA) control charts, have also been extended for monitoring linear drifts. For example, Davis and Woodall (1988) considered the Shewhart chart supplemented with run rules under a linear drift. Davis and Krehbiel (2002) investigated the performance of Shewhart and zone charts under linear trends. Rainer et al. (2001)

* Corresponding author.
E-mail addresses: ljshu@umac.mo (L. Shu), ktsui@isye.gatech.edu (K.-L. Tsui).

0167-9473/$ – see front matter © 2011 Elsevier B.V. All rights reserved.
doi:10.1016/j.csda.2011.04.008

suggested Shewhart-type UMP charts derived from the uniformly most powerful (UMP) test for monitoring linear drifts. Based on a modification of the Markov chain method developed by Brook and Evans (1972) and Bissell (1984) proposed methods for computing average run length (ARL) of CUSUM charts under linear drifts in the process mean. However, this procedure did not produce accurate ARL values. Gan (1992, 1996) further presented an accurate numerical method based on an integral equation for computing the ARL of CUSUM charts under linear trends. Koning and Does (2000)developed a CUSUM-type chart from the UMP test for the detection of linear trend. In addition to the use of Shewhart and CUSUM charts, Gan (1991) and Reynolds and Stoumbos (2001) considered the EWMA chart for detecting linear drifts. Other monitoring schemes for detecting linear drifts are given by Domangue and Patch (1991), Runger and Testik (2003), Fahmy and Elsayed (2006a,b) and Tseng et al. (2007).

Recently, Zou et al. (2009) made a comprehensive comparison among various control charts under linear drifts, including CUSUM, EWMA, generalized EWMA (GEWMA) and generalized likelihood ratio test (GLRT). They showed that the GLRT method can provide the best average performance at both small and large drifts in the process mean, and that the EWMA chart outperforms the CUSUM chart under linear drifts. Compared to the EWMA method, the GLRT method has slightly worse performance for detecting small linear drifts but much better performance for detecting large drifts. However, the GLRT procedure does not have recursive form and suffers from the computation load issue.

The literature on the efficiency and robustness of the EWMA chart for monitoring step mean shifts indicates that it is efficient in detecting small shifts in the process mean but not efficient for large mean shifts, as compared to the conventional Shewhart control charts. Yashchin (1995) investigated the estimation efficiency of the EWMA scheme in terms of an inertia function. He showed that the inertia increases as the magnitude of the mean shift increases. Therefore, the EWMA statistic with a small smoothing constant is not efficient in estimating abrupt mean changes of moderate and large magnitudes. This phenomenon has been referred to as the "inertia problem" (Woodall and Mahmoud, 2005). The inertia phenomenon occurs when the value of the EWMA statistic is on the lower side of the control limits but the shift occurs toward the opposite direction. In this case, if the smoothing constant is small, it takes a longer time for the EWMA statistic to exceed the control limits.

The inertia problem of the EWMA chart can be counteracted in part by using the combined Shewhart–EWMA chart (Lucas and Saccucci, 1990). However, the Shewhart–EWMA chart is not a smooth combination of the Shewhart principle and the EWMA scheme. To better overcome this problem, Yashchin (1995) proposed a smooth combination based on the adaptive EWMA (AEWMA) scheme. The underlying idea of the AEWMA procedure is to allocate the weight on past observations at each time step according to the magnitude of the estimation error. Unlike the conventional EWMA method, the smoothing constant used in the AEWMA scheme is no longer constant but varies over time. This weighting scheme has been widely discussed in the SPC literature recently. See, for example, Capizzi and Masarotto (2003), Shu (2008), Shu et al. (2008), Mahmoud and Zahran (2010) and Tseng et al. (2010).

Similarly, the EWMA chart for monitoring linear drifts also suffers from the inertia problem when the drift coefficient in the mean is large. In this article we extend the AEWMA scheme for monitoring linear drifts in the process mean. Markov chain, integral equation, and Monte Carlo simulations have been widely used to evaluate performance of a control chart. Similar to the approach of Gan (1991), an integral equation approach was developed to evaluate the performance of the AEWMA chart under linear drifts. This numerical approach allows for a quick analysis of the chart performance without running a large number of simulations. The AEWMA statistic can be expressed in an iterative way and thus can be viewed simpler in format than the GLRT procedure.

The rest of the paper is organized as follows. In Section 2, the AEWMA chart for monitoring linear drifts is introduced. In Section 3, the integral equation procedure for approximating the ARL of the AEWMA chart is developed. In Section 4, the approximation accuracy of the integral equation approach is evaluated. In Section 5, the performance of the AEWMA chart is compared with various control charts. In Section 6, a sequential design procedure is proposed to facilitate the implementation of AEWMA charts. Finally, some concluding remarks are given.

2. The AEWMA chart under linear drifts

Let $X_1, X_2, \ldots$, be a sequence of observations collected at fixed intervals of time. When the process is in the state of statistical control, observations are assumed to be independently distributed from a normal distribution with a known mean μ_0 and known variance σ_0^2. After an unknown time point τ, the process mean is subject to a linear drift while the variance remains unchanged. The amount of drift is $\theta\sigma_0$ per unit time, where θ is unknown. In other words, the process mean at time t can be represented as

$$E(X_i) = \begin{cases} \mu_0, & i \le \tau \\ \mu_0 + \theta\sigma_0(i-\tau), & i > \tau. \end{cases}$$

Without loss of generality, we will assume the in-control process mean to be zero and the standard deviation to be one, i.e., $\mu_0 = 0$ and $\sigma_0^2 = 1$. Furthermore, we assume $\tau = 0$ to simplify the discussion. These assumptions are consistent with those made in Gan (1991). The ARL obtained assuming $\tau = 0$ has been referred to as the zero-state ARL while the ARL computed based on $\tau > 0$ has been called the steady-state ARL. Within our investigations, both the zero-state and steady-state results would provide qualitatively the same conclusion. For the sake of simplicity, we only consider the zero-state ARL performance in this paper while the steady-state ARL performance can be similarly analyzed.

The EWMA statistics are

$$Q_t = \lambda X_t + (1-\lambda)Q_{t-1}, \quad t = 1, 2, \ldots \tag{1}$$

where λ is a smoothing constant, $\lambda \in (0, 1]$. The initial value, Q_0, is usually set at zero but other positive values could be chosen if fast initial response of the EWMA chart is desired (Lucas and Crosier, 1982). An out-of-control signal is triggered when $|Q_t| > h_1$, where $h_1 = c_1\sqrt{\lambda/(2-\lambda)}$. From Eq. (1), it can be seen that more weight is given to past observations as λ gets closer to 0, which results in better sensitivity to the detection of small shifts. On the other hand, a larger λ tends to provide better sensitivity to the detection of larger shifts. However, a single EWMA chart cannot perform relatively well at both small and large shifts.

To improve the detection performance of EWMA schemes, the AEWMA method with a varying smoothing parameter has been suggested (Yashchin, 1995). The AEWMA statistics have the form

$$G_t = G_{t-1} + \phi(e_t), \quad t = 1, 2, \ldots \tag{2}$$

where $e_t = X_t - G_{t-1}$ is the prediction error, and $\phi(\cdot)$ is a score function. The initial value G_0 is set to $G_0 = 0$. It is interesting to note that when $e_t \neq 0$, the AEWMA statistic can be rewritten as

$$G_t = (1 - w(e_t))G_{t-1} + w(e_t)X_t,$$

where $w(e_t) = \phi(e_t)/e_t$. When $\phi(e) = \lambda e$, the AEWMA statistics in Eq. (2) reduce to the conventional EWMA statistics. An out-of-control signal is alarmed on the AEWMA chart when $|G_t| > h_2$, where $h_2 = c_2\sqrt{\lambda/(2-\lambda)}$.

In the AEWMA scheme, the weight put on the most recent observation, $w(e_t)$, is updated based on the estimation error. Yashchin (1995) suggested using some weight functions motivated by robust procedures such as Huber's function (Huber, 1981) and Welsch's function (Holland and Welsch, 1977). In this paper, for the sake of simplicity, we restrict our discussion to Huber's score function

$$\phi_{\text{hub}}(e) = \begin{cases} e + (1-\lambda)\gamma, & e < -\gamma \\ \lambda e, & |e| \le \gamma \\ e - (1-\lambda)\gamma, & e > \gamma, \end{cases} \tag{3}$$

while other weight functions can be similarly discussed. The reasonable choice of γ (in the unit of σ_0) is on the interval [2.5, 4] (Capizzi and Masarotto, 2003). When $\gamma \to \infty$, $w_{\text{hub}}(e) = \phi_{\text{hub}}(e)/e = \lambda$, and the AEWMA charts performs the same as the conventional EWMA chart. When the forecast error is large (i.e., $e_t \to \infty$), $w_{\text{hub}} \to 1$, and the AEWMA chart performs essentially like the Shewhart chart in the case. Therefore, the AEWMA chart can be viewed as a smooth combination of the Shewhart and EWMA charts.

3. The ARL integral equation for the AEWMA chart under linear drifts

Similar to the approach of Gan (1991), the integral equation procedure can be used to approximate the ARL values of AEWMA control charts under linear drifts. Define $L_j(v)$ as the ARL of the two-sided AEWMA control chart starting from $G_j = v$. Let μ_0 be the in-control mean. Assuming $\tau = 0$, denote $\mu_1, \ldots, \mu_{m-1}, \mu_m, \mu_{m+1} \ldots$ be the respective process means at $t = 1, \ldots, m-1, m, m+1, \ldots$. Note that μ_m can be set to an arbitrary large number to approximate a linear drift process. When μ_m is sufficiently large, any control chart would signal the drift immediately after m steps, namely, $L_j(v) = 1$ for $j > m$. For this reason, one can simply view μ_m as the stabilized mean as done in Gan (1991), i.e., $\mu_{m+i} = \mu_m$ for $i = 1, 2, \ldots$, although this is not exact. By doing so, one can achieve certain simplicity when deriving the ARL integral equation of the AEWMA chart.

Given $G_j = v$ for arbitrary $v \in (-h_2, h_2)$, $G_{j+1} = v + \phi(X_{j+1} - v)$ based on Eq. (2). If $|G_{j+1}| > h_2$, an out-of-control signal is issued. Otherwise if $-h_2 < G_{j+1} < h_2$, the AEWMA control chart continues from $G_{j+1} = v + \phi(X_{j+1} - v)$ with an additional ARL of $L_{j+1}(v + \phi(X_{j+1} - v))$. Define $f_{\mu_{j+1}}(x)$ as the probability density function (PDF) of a normal distribution with mean μ_{j+1}. Then, for $j = 0, 1, \ldots, m-1$, we obtain the following recursive equation for the ARL function

$$L_j(v) = 1 \cdot \Pr(|v + \phi(X_{j+1} - v)| \ge h_2) + \int_{|v+\phi(X_{j+1}-v)|<h_2} [1 + L_{j+1}(v + \phi(x - v))] f_{\mu_{j+1}}(x) \mathrm{d}_x. \tag{4}$$

By defining $g = v + \phi(X_{j+1} - v)$, one can solve for $X_{j+1} = v + \phi^{-1}(g - v)$, where $\phi^{-1}(\cdot)$ denotes the inverse of the score function. Then Eq. (4) can be rewritten as

$$L_j(v) = 1 + \int_{-h_2}^{h_2} L_{j+1}(g) f_{\mu_{j+1}}(v + \phi^{-1}(g - v))[\phi^{-1}(g - v)]' \mathrm{d}_g,$$

where $[\phi^{-1}(g - v)]'$ is the derivative of $\phi^{-1}(g - v)$ with respect to g. For $j = m$, the ARL function $L_m(v)$ can be similarly expressed as

$$L_m(v) = 1 + \int_{-h_2}^{h_2} L_m(g) f_{\mu_m}(v + \phi^{-1}(g - v))[\phi^{-1}(g - v)]' \mathrm{d}_g. \tag{5}$$

Table 1
Approximation to the in-control ARL of the AEWMA chart based on different values of N when $\lambda = 0.1$, $\gamma = 3$, and $c_2 = 2.542$.

N	21	51	101	151	201	251	301	501	1001
ARL_0	178	197	195	203	200	198	200	200	200

When Huber's score function in Eq. (3) is used for the AEWMA chart, one can obtain the following inverse function

$$\phi_{\text{hub}}^{-1}(y) = \begin{cases} y - (1-\lambda)\gamma, & y < -\lambda\gamma \\ y/\lambda, & |y| \le \lambda\gamma \\ y + (1-\lambda)\gamma, & y > \lambda\gamma. \end{cases}$$

Note that $\phi_{\text{hub}}^{-1}(g - v)$, is not differentiable at $g = v \pm \lambda\gamma$; however, the value of $(g - v)$ will not be exactly equal to $\lambda\gamma$ in general. For this reason, we simply express $[\phi^{-1}(g - v)]'$ as

$$\frac{\mathrm{d}[\phi_{\text{hub}}^{-1}(g-v)]}{\mathrm{d}g} = \begin{cases} 1, & g - v < -\lambda\gamma \\ 1/\lambda, & |g - v| \le \lambda\gamma \\ 1, & g - v > \lambda\gamma. \end{cases}$$

Eq. (5) is an integral equation and can be approximated numerically by the Nyström method, which is a well-known tool for solving integral equations (Baker, 1977; Hackbusch, 1995). The main idea of the Nyström method is simple and leads to excellent results for proper integral kernels. The integral can be replaced by an appropriate quadrature like Gauss–Legendre quadrature, and the ARL function can then be approximated numerically by solving a system of linear equations. Based on the numerical analysis literature (Hackbusch, 1995), the Gauss–Legendre Nyström methods with proper integral kernel provide good accuracy. Similar to the method of Gan (1991), the Gauss–Legendre Nyström method was used to approximate the integral equation in this paper.

Let $(v_1, v_2, \ldots, v_N)$ and $(w_1, w_2, \ldots, w_N)$ be the Gauss–Legendre abscissas and weights for the range of integration $(-h_2, h_2)$. The resulting linear system of equations to Eq. (5) is given by

$$L_m(v_i) = 1 + \sum_{j=1}^{N} w_j L_m(v_j) f_{\mu_m}(v_i + \phi^{-1}(v_j - v_i))[\phi^{-1}(v_j - v_i)]' \tag{6}$$

for $i = 1, 2, \ldots, N$. Define $\mathbf{\Omega}_m$ as an N-dimensional square matrix whose element in row i and column j is

$$\Omega_{mij} = w_j f_{\mu_m}(v_i + \phi^{-1}(v_j - v_i))[\phi^{-1}(v_j - v_i)]'.$$

Thus, using Gaussian quadrature rules, Eq. (5) may be replaced by

$$\mathbf{L}_m = \mathbf{1} + \mathbf{\Omega}_m \mathbf{L}_m,$$

where $\mathbf{L}_m$ is the N-dimensional column vector whose element in row i is $L_{mi} = L_m(v_i)$, and $\mathbf{1}$ is a column vector of ones. After solving this linear system of equations, we are able to evaluate $L_m(v)$ for arbitrary $v \in (-h_2, h_2)$. Once $L_m(v)$ was obtained, simple backward substitution can be employed to solve Eq. (4) for $L_j(v)$ recursively, for $j = m-1, m-2, \ldots, 1, 0$. The ARL of an AEWMA chart starting with $G_0 = 0$ is approximated by $L_0(0)$.

4. Computational aspects and approximation accuracy

The algorithm in Section 3 has been implemented in a Matlab program that uses the routine "normcdf" to compute the cumulative distribution function (CDF) of a normal distribution. In the in-control situation, $\mu_j = \mu_0$ for all j. Thus, the in-control ARL, ARL_0, can be approximated based on Eq. (6) by replacing μ_m with μ_0, which does not require m backward iterations. However, to approximate the out-of-control ARL, ARL_1, one needs to employ m-step iterations from the calculation of $L_m(v)$ to $L_0(0)$. Clearly, the load for the computation of ARL_1 would be heavier than the computation of ARL_0.

As an example, Table 1 shows the approximation to the in-control ARL of the AEWMA chart computed using different values of N when $\lambda = 0.1$, $\gamma = 3$, and $c_2 = 2.542$. The experiment suggests that satisfactory results can be obtained by choosing N to be larger than 50. In this paper, we prefer to use a large value of $N = 501$ to approximate the ARL_0 of AEWMA charts. This helped us obtain the ARL_0 approximation with a reasonable accuracy while only increasing the computation load slightly based on computation capability of modern computers. The execution time is within 6 s on a personal Pentium 4 computer with CPU processor 2.18 GHz.

The accuracy of approximating the ARL_1 values by the integral equation approach was assessed by comparing the approximated ARL with the simulated ARL values based on a large number of simulation runs. The approximated ARL_1 converged as the constant m increases. The value of m used to stabilize the ARL_1 approximation increases as the drift coefficient, θ, decreases. A relatively large value of m is required when θ is small. For example, as shown in Gan (1991),

Table 2
Approximation to the out-of-control ARL of the AEWMA chart based on different values of N and m when $\lambda = 0.1$, $\gamma = 3$, and $c_2 = 2.542$.

θ	Simulated		$N = 51$				$N = 101$			
	ARL	SDRL	$m = 6$	30	150	700	6	30	150	700
0.001	133.71	87.93	197.04	192.22	146.02	132.85	195.15	190.43	145.19	132.27
0.002	102.39	57.53	196.37	178.65	104.37	102.03	194.50	177.14	104.06	101.75
0.005	66.29	30.16	191.83	121.84	66.06	66.06	190.04	121.21	65.98	65.98
0.01	45.66	17.83	177.21	63.97	45.58	45.58	175.70	63.85	45.56	45.56
0.05	18.27	5.13	53.66	18.26	18.26	18.26	53.57	18.27	18.27	18.27
0.1	12.31	3.04	20.51	12.31	12.31	12.31	20.51	12.31	12.31	12.31
0.2	8.34	1.84	9.49	8.33	8.33	8.33	9.50	8.34	8.34	8.34
0.5	4.98	1.02	4.98	4.98	4.98	4.98	4.99	4.98	4.98	4.98
1	3.32	0.73	3.31	3.31	3.31	3.31	3.32	3.32	3.32	3.32
2	2.10	0.54	2.08	2.08	2.08	2.08	2.10	2.10	2.10	2.10
3	1.61	0.49	1.57	1.57	1.57	1.57	1.62	1.62	1.62	1.62

the constant $m = 700$, 150, 30, and 6 can provide a stabilized ARL_1 approximation of an EWMA chart for drift coefficients $\theta = 0.001$, 0.01, 0.1 and 1, respectively. These specific m values for different drift coefficients were determined in Gan (1991) by gradually increasing m until the ARL_1 values obtained did not change appreciably.

For illustration, Table 2 shows the approximation to the ARL_1 values of the AEWMA chart computed using different values of N and m, where again $\lambda = 0.1$, $\gamma = 3$, and $c_2 = 2.542$. The simulated ARL_1 value and the standard deviation of run length (SDRL) are given in columns 2 and 3 of Table 2, respectively. The simulation was conducted based on 10^6 replications. From Table 2, the suggested m value by Gan (1991) to stabilize ARL_1 values also applies to the AEWMA chart here. For example, when $N = 51$, the use of m greater than 150 can provide the stabilized ARL_1 value of 45.58 when $\theta = 0.01$, and the use of m greater than 6 gives the stabilized ARL_1 value of 3.31 when $\theta = 1$. These observations indicate that the ARL results approximated by the integral equation procedure match the simulation results very well.

Note that the computation load increases as N and m increase when approximating the ARL_1 values of AEWMA control charts using the integral equation procedure. To provide a reasonable accuracy while not increasing computation load remarkably, one can use the combination of a larger N value ($N = 101$) and a smaller m ($m = 150$) value to approximate the ARL_1 for a relatively large drift coefficient, say, $\theta \geq 0.05$. On the other hand, when drift coefficient is relatively small, say, $\theta < 0.05$, one can use the combination of a smaller N value ($N = 51$) and a larger m value ($m = 700$) to approximate the ARL_1. With the increasing capabilities of modern computers, we have not found that the computation load was overly burdensome, even for the case with $N = 101$ and $m = 700$. The execution time on a personal computer is usually of the order of a few minutes for the computation of ARL_1 values.

5. Performance comparisons

In this section, the ARL performance of AEWMA control charts is compared with the traditional EWMA chart under a linear drift in the mean. Moreover, the AEWMA chart is compared with some alternatives being able to provide a balanced detection performance against changes of different magnitudes, including the combined Shewhart–EWMA chart, the GEWMA chart, and the GLRT method.

5.1. Comparison with EWMA charts

Table 3 compares the zero-state ARL of AEWMA charts with the traditional EWMA chart under a linear drift in the process mean. The integral equation procedure was used to calculate the ARL values of both the EWMA and AEWMA charts. For illustration, the value of $\lambda = 0.059$ was considered for both the EWMA and AEWMA charts. Both charts are designed to have a zero-state ARL_0 of 200. The EWMA chart with $\lambda = 0.059$ is optimal at detecting a linear drift with coefficient of $\theta = 0.01$, according to Gan (1991). From Table 3, it is not surprising to see that the EWMA chart has the smallest ARL_1 at $\theta = 0.01$.

Note that when $\gamma \geq 4$, the ARL performance of the AEWMA chart is nearly the same as that of the EWMA chart for $\theta \leq 0.5$. This is because when γ takes a large value, the estimation errors are very unlikely to exceed γ when the drift is not large. In this case, the AEWMA scheme performs essentially the same as the regular EWMA scheme. A pronounced observation from Table 3 is that when γ decreases, the AEWMA chart can perform substantially better than the EWMA chart at large drift coefficients and closely to the latter at small drift coefficients. For example, when γ decreases from $\gamma = 5$ to $\gamma = 3$, the percentage decrease in the ARL_1 at $\theta = 2$ is as large as 22.7% $((2.11 - 2.73)/2.73)$ while the percentage increase in the ARL_1 at $\theta = 0.01$ is 1.65% $((45.00 - 44.27)/44.27)$ only.

The above observations demonstrate the benefit of introducing the additional parameter γ for the AEWMA chart for detecting linear drifts in the process mean. In particular, the parameter γ can be managed to improve the performance of an AEWMA chart at larger drifts by a large percentage with only minor loss in the efficiency in detecting smaller drifts in the mean. This agrees with the expectation of the superiority of AEWMA estimators over conventional EWMA statistics in catching up with large shifts in the level of process mean.

Table 3
ARL values of AEWMA charts under linear drifts when $\lambda = 0.059$.

θ	AEWMA						EWMA
	γ	2.5	3.0	3.5	4.0	4.5	5.0	$c_1 = 2.277$
	$c_2 =$	3.046	2.395	2.296	2.280	2.278	2.277	
0.000		200.0	200.1	200.0	200.1	200.1	199.8	199.8
0.001		145.7	128.4	127.9	127.8	127.9	127.7	127.7
0.002		113.2	98.6	97.7	97.5	97.5	97.5	97.5
0.005		73.6	64.4	63.6	63.4	63.4	63.4	63.4
0.01		50.82	45.00	44.39	44.30	44.29	44.27	44.27
0.05		20.46	18.75	18.54	18.51	18.51	18.51	18.51
0.1		13.76	12.84	12.72	12.71	12.71	12.71	12.71
0.2		9.16	8.79	8.76	8.76	8.77	8.77	8.77
0.5		5.10	5.25	5.35	5.39	5.41	5.41	5.41
1.0		3.13	3.41	3.62	3.73	3.77	3.79	3.79
2.0		1.91	2.11	2.31	2.51	2.63	2.70	2.73
3.0		1.49	1.62	1.76	1.89	1.98	2.03	2.06
4.0		1.15	1.24	1.38	1.56	1.73	1.88	2.00

Table 4
ARL comparisons between the combined Shewhart–EWMA and AEWMA charts under linear drifts.

θ	$\lambda = 0.059$			$\lambda = 0.10$			$\lambda = 0.15$		
c_1/c_2	Shewhart–EWMA		AEWMA	Shewhart–EWMA		AEWMA	Shewhart–EWMA		AEWMA
	SCL = 3.5	SCL = 4.0	$\gamma = 3$	SCL = 3.5	SCL = 4.0	$\gamma = 3$	SCL = 3.5	SCL = 4.0	$\gamma = 3$
	2.312	2.282	2.395	2.485	2.457	2.542	2.595	2.572	2.64
0	200.2	200.0	200.1	200.0	199.9	199.8	199.7	200.2	199.8
0.0005	158.0	**157.2**	158.6	160.9	**159.9**	162.5	165.0	**164.3**	165.9
0.001	128.0	**127.4**	128.4	132.4	**131.6**	132.3	136.7	**136.1**	138.2
0.005	63.66	**63.38**	64.40	65.07	**64.81**	65.98	67.72	**67.27**	68.60
0.01	44.48	**44.33**	45.00	45.12	**44.86**	45.56	46.51	**46.30**	47.03
0.05	18.61	**18.55**	18.75	18.15	**18.08**	18.27	18.08	**17.99**	18.24
0.1	12.74	**12.73**	12.84	12.23	**12.19**	12.31	12.01	**11.97**	12.10
0.5	5.31	5.38	**5.25**	5.01	5.04	**4.98**	4.78	4.81	**4.78**
1	3.55	3.70	**3.41**	3.39	3.47	**3.32**	3.24	3.29	**3.21**
2	2.22	2.45	**2.11**	2.19	2.33	**2.10**	2.13	2.22	**2.08**
3	1.70	1.86	**1.62**	1.69	1.85	**1.62**	1.69	1.84	**1.62**
4	1.31	1.50	**1.24**	1.31	1.50	**1.24**	1.30	1.50	**1.24**

5.2. Comparison with other charts

For the detection of step shifts or linear drifts, the EWMA control chart is often designed to optimize a pre-specified value of the change. However, the magnitude of the shift occurred in the future is often unknown. In order to provide a balanced detection performance against shifts of different magnitudes, different methods have been suggested for monitoring step mean shifts. It is also straightforward to extend them to the monitoring of linear drifts in the process mean.

An intuitive way to achieve an overall good detection performance against a range of shifts is based on a multi-chart approach, which involves the use of more than one control chart simultaneously. The simplest way to do this is perhaps to combine the Shewhart chart with the EWMA chart (Lucas and Saccucci, 1990). This scheme is achieved by adding Shewhart limits to an EWMA scheme. An out-of-control signal is triggered on the combined Shewhart–EWMA chart whenever $|Q_t| > c_1\sqrt{\lambda/(2-\lambda)}$ or $|X_t| >$ SCL, where SCL denotes the width of the Shewhart control limit. The value of SCL is often set to be a relatively large value so that it has only slight effect on the detection performance at small shifts. The values of SCL $= 4.0$ and 3.5 were considered here, which have been often suggested for the practical design of the combined Shewhart–EWMA chart (Lucas and Saccucci, 1990). As suggested by a referee, some different values of λ were selected for both the combined Shewhart–EWMA and AEWMA charts, including $\lambda = 0.059$, 0.1, and 0.15. The value of $\gamma \in [2.5, 4]$ for the AEWMA chart was set to $\gamma = 3$. The ARL_0 values of both charts were maintained as 200.

Table 4 compares the ARL values between the combined Shewhart–EWMA and AEWMA charts under linear drifts. For a given λ value, the smallest ARL_1 value between the Shewhart–EWMA and AEWMA charts at a particular drift coefficient was denoted in bold. It is known that the combined Shewhart–EWMA chart with larger SCL value is less sensitive to the detection of large shifts but more sensitive to the detection of small shifts. As expected, it can be seen from Table 4 that for a given λ value, the combined Shewhart–EWMA chart with SCL $= 4$ has larger ARL_1 values at relatively large drifts (say $\theta \geq 0.5$) than the same chart with SCL $= 3.5$ but smaller ARL_1 values for $\theta \leq 0.1$.

When comparing the AEWMA chart with the combined Shewhart–EWMA chart, it can be seen from Table 4 that no one chart can perform uniformly better than the other. In general, the AEWMA chart with $\gamma = 3$ has smaller ARL_1 values for $\theta \geq 0.5$ than the combined Shewhart–EWMA charts but larger ARL_1 values for $\theta \leq 0.1$. However, it is interesting to note

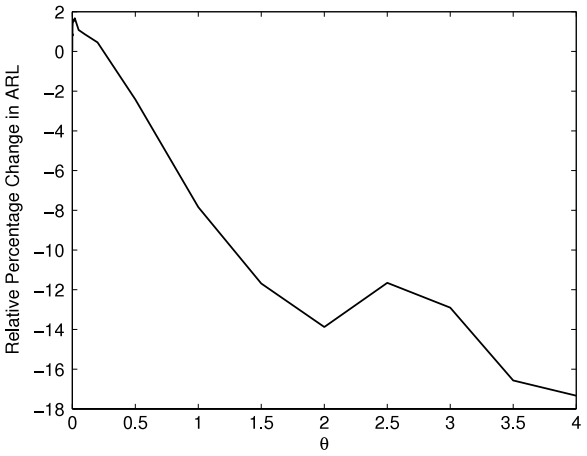

Fig. 1. ARL percentage changes of the AEWMA chart relative to the combined Shewhart–EWMA chart with $\lambda = 0.059$ and SCL $= 4$.

that the relative efficiency loss of the AEWMA chart at small drift coefficients is negligible but the relatively efficiency gain at large drift coefficients is remarkable, as compared to the combined Shewhart–EWMA chart. This result is similar to that under the case with step shifts in the process mean, which was studied by Capizzi and Masarotto (2003) and Simões et al. (2010). To illustrate this, Fig. 1 further plots the ARL percentage changes of the AEWMA chart relative to the combined Shewhart–EWMA chart based on $\lambda = 0.059$ and SCL $= 4$. It is clear that when compared to the Shewhart–EWMA chart, the relative ARL percentage increase of the AEWMA chart for $\theta \leq 0.1$ is only within 2% but the relative ARL percentage decrease can be as large as 17%. In this sense, the AEWMA chart can provide a slightly better overall performance than the Shewhart–EWMA chart.

The other ways to provide an overall good detection performance involve the use of more sophisticated control charts, including the GEWMA chart and the GLRT method. The GEWMA chart proposed by Han and Tsung (2004) is based on

$$T_{\mathrm{GEWMA}}(t) = \max_{1\leq k\leq t} W_t\left(\frac{1}{k}\right),$$

where

$$W_t(\lambda) = \sqrt{\frac{2-\lambda}{\lambda[1-(1-\lambda)^{2t}]}} \sum_{i=1}^{t} \lambda(1-\lambda)^{t-i} X_i.$$

Based on the maximum likelihood estimate of the drift coefficient, Zou et al. (2009) developed the following GLRT for detecting linear drifts

$$T_{\mathrm{GLRT}}(t) = \max_{1\leq k\leq t} \frac{1}{a_k} V_k^t, \tag{7}$$

where $V_k^t = \sum_{i=t-k+1}^{t}(i-t+k)X_i$ and $a_k = \left[\sum_{i=t-k+1}^{t}(i-t+k)^2\right]^{1/2} = \sqrt{k(k+1)(2k+1)/6}$. Aimed at detecting a positive drift in the mean, Zou et al. (2009) considered the upper-sided form by simply removing the lower control limit from a control chart. The one-sided upper GEWMA and GLRT charts trigger an out-of-control signal when $T_{\mathrm{GEWMA}}(t) > h_3$ and $T_{\mathrm{GLRT}}(t) > h_4$, respectively.

For fair comparisons, the AEWMA chart in Eq. (2) is modified into the one-sided upper form by similarly removing the lower control limit. That is, the upper AEWMA chart signals when $G_t > c_2\sqrt{\lambda/(2-\lambda)}$. As done in Zou et al. (2009), the ARL_0 value for all the charts were maintained around 1730. Again, the AEWMA chart based on $\lambda = 0.059$ and $\gamma = 3.5$ was considered here. To maintain the same in-control ARL of 1730, the control limits for the upper-sided AEWMA, GEWMA, and GLRT charts are given by $c_2 = 2.926$, $h_3 = 3.500$, and $h_4 = 3.580$, respectively. Table 5 compares the ARL values of the upper GEWMA, GLRT, and AEWMA charts under linear drifts. The ARL values for the GEWMA and GLRT charts are adopted from Table 1 of Zou et al. (2009).

From Table 5, the GEWMA chart performs closely to the GLRT chart. The AEWMA chart performs better than both the GEWMA and GLRT charts for $\theta \leq 0.05$ but slightly worse for $\theta > 0.1$. These results indicate that no one chart can perform uniformly better than the other control charts. However, the AEWMA charting statistic has the recursive form while the GLRT and GEWMA methods have more complicated form. Note that the GLRT cannot be written in the recursive form. The GEWMA chart needs to compute t different EWMA statistics at each time step. As a result, both the GEWMA and GLRT methods suffer from extensive computation load when the time, t, goes to infinity. In this sense, the AEWMA chart is simple to implement as compared to the GEWMA and GLRT methods. When the ARL_0 value was approximately maintained

Table 5
ARL comparisons among the GEWMA, GLRT and AEWMA charts under linear drifts when $ARL_0 = 1730$.

θ	GEWMA $h_3 = 3.50$	GLRT $h_4 = 3.58$	AEWMA $c_2 = 2.926$
0.0005	368	375	349
0.001	249	252	234
0.005	95.4	96.2	87.07
0.01	62.0	62.1	56.58
0.05	22.5	22.4	21.72
0.1	14.5	14.4	14.66
0.5	5.18	5.10	5.98
1	3.31	3.26	3.91
2	2.12	2.09	2.37
3	1.72	1.69	1.80
4	1.34	1.31	1.42

as 200, similar observations can be made. For the sake of simplicity, the results based on $ARL_0 = 200$ were not presented here.

6. Design of AEWMA charts

The design of an AEWMA chart is a three-degree-of-freedom problem, which involves the selection of parameters λ, γ, and c_2. In order to provide some insights into the choice of chart parameters, the effects of parameters λ and γ are first investigated. Then, a sequential design procedure is proposed to design an AEWMA chart for the purpose of providing an overall good detection performance at both a small drift and a large drift in the process mean.

To better understand the joint effects of λ and γ on the performance of the AEWMA chart under linear drifts, Fig. 2 shows contour plots of the ARL_1 values of the AEWMA chart as a function of λ and γ under a range of drift coefficients, $\theta = 0.01$, 0.05, 0.10, and 0.25, where $ARL_0 = 200$. A pronounced observation from Fig. 2 is that when $0.01 \leq \theta \leq 0.25$, the ARL_1 contours are nearly vertical over the range $3.5 \leq \gamma \leq 5.0$. This indicates that the choice of $\gamma \in [3.5, 5]$ has less effect on the detection performance when the drift coefficient is small, which in turn implies that an appropriate γ value can be selected to tune the chart performance at large drifts with negligible loss of performance at small drifts. This good property of the parameter γ has also been illustrated in Table 3.

Moreover, it can be observed from Fig. 2 that as θ increases from 0.01 to 0.25, the λ value for providing the minimum ARL_1 value tends to increase. This implies that small λ values are more sensitive to drifts of small magnitudes. To sum up, small values of λ and large values of γ tend to improve the detection performance of AEWMA charts at small drifts while large values of λ and small values of γ values tend to improve the detection performance at large drifts. This is consistent with the result of AEWMA chart under step mean changes, as investigated by Capizzi and Masarotto (2003).

Capizzi and Masarotto (2003) proposed a two-step procedure to jointly search the optimal parameters of an AEWMA chart for efficiently detecting a small shift and a large shift in the process mean. Similarly, a two-step procedure can be followed to design an AEWMA chart for monitoring processes subject to linear drifts. However, note that Capizzi and Masarotto's procedure is a joint searching procedure. It requires extensive computation work and is thus complicated. Rather, a sequential searching procedure is employed here for finding the nearly "optimal" parameters. The sequential searching procedure requires less computation work while providing a relatively good performance under linear drifts with both small and large drift coefficients.

In the sequential searching procedure, the optimal λ value of an EWMA chart for detecting a specified small drift coefficient is first determined. Due to the attractive property that the parameter γ can be managed to improve the detection performance at large drifts by a large percentage while causing a slight loss in the detection performance at small drifts, this optimal λ value for the EWMA chart can be also considered approximately optimal for the AEWMA chart. After the optimal λ value is determined, the γ value is obtained to optimize the detection performance of the AEWMA chart at a specified large drift coefficient. Details of the sequential searching procedure for the AEWMA chart under linear drifts are summarized below:

(i) Choose a desired ARL_0, and determine the interval of drift coefficients to be detected, $[\theta_1, \theta_2]$.
(ii) For the specified ARL_0, find the value of λ giving the minimum ARL_1 of an EWMA chart at θ_1. Some of the optimal λ values can be found in Gan (1991).
(iii) Select a small positive constant α (e.g., $\alpha = 0.05$) to control the efficiency loss at θ_1 due to the introduction of the parameter γ.
(iv) Based on the ARL_0 value and the optimal λ value obtained in step (ii), search the optimal γ value having the minimum ARL at θ_2 subject to the condition that the percentage increase in the ARL_1 at θ_1 is at most α.

Tables 6–8 report a list of parameters of AEWMA charts under linear drifts in the mean for a range of in-control ARL values. These parameters are adequate for most practical purposes, and are obtained using the forgoing strategy through the above integral equation approximation. From Tables 6–8, it can be observed that for a fixed θ_1 value, the optimal λ value

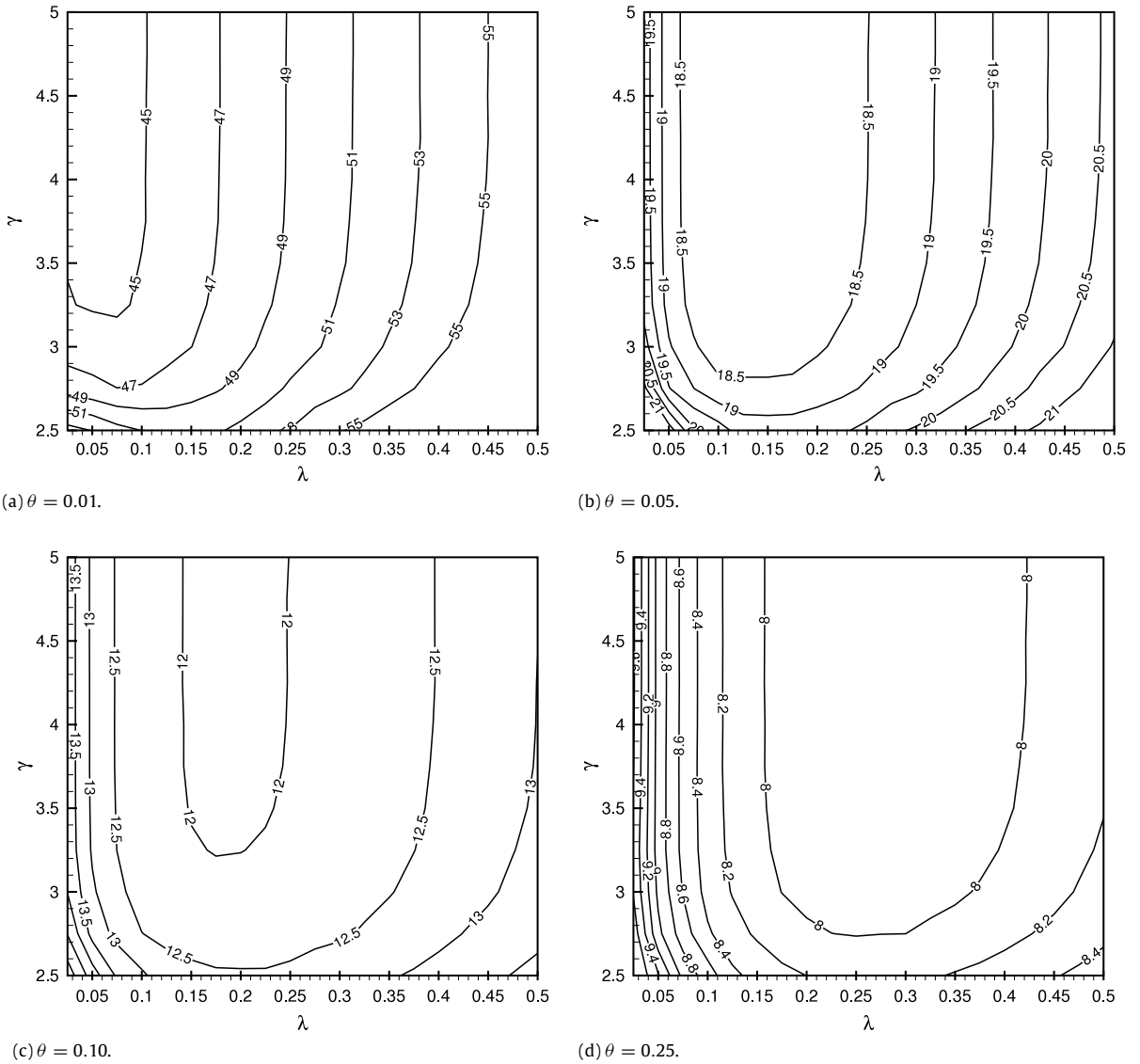

Fig. 2. Contour plots of ARL_1 values of the AEWMA chart under linear drifts based on $ARL_0 = 200$ when (a) $\theta = 0.01$; (b) $\theta = 0.05$; (c) $\theta = 0.10$; and (d) $\theta = 0.25$.

decreases as the target in-control ARL increases. For example, when ARL_0 increases from $ARL_0 = 200$ to $ARL_0 = 1000$, the optimal λ value at $\theta_1 = 0.01$ decreases from 0.074 to 0.043. Another tendency is that for a fixed ARL_0, the optimal λ value increases as θ_1 increases while the optimal γ value decreases as θ_2 increases.

As an example, suppose that the desired in-control ARL is $ARL_0 = 200$, and that the interval of drift coefficients of interest in the mean to be detected is [0.01, 0.05]. From Table 10 in Gan (1991), the optimal value of λ of an EWMA chart at $\theta_1 = 0.01$ is $\lambda = 0.059$, giving the minimum ARL_1 of 44.27. If $\alpha = 0.05$, the optimal γ value is searched on the range $2.5 \leq \gamma \leq 4$ with a step size of 0.05 for minimizing the ARL_1 at $\theta_2 = 0.05$, subject to the condition that the ARL_1 value of the AEWMA chart at $\theta_1 = 0.01$ is no more than 46.48 (i.e., $(1 + 0.05) \cdot 44.27$). The value of $\gamma = 3.85$ gives the minimum ARL_1 at $\theta_2 = 0.05$ of 18.53 and an out-of-control ARL of 44.35 at $\theta_1 = 0.01$. Thus, the combination ($\lambda = 0.059$, $\gamma = 3.85$, $c_2 = 2.281$) shown in Table 6 is considered to be nearly "optimal" for detecting linear drifts with coefficients on the range [0.01, 0.05]. The same approach can be used to determine the nearly optimal parameters of AEWMA charts for other cases.

7. Concluding remarks

The AEWMA procedure is a generalization of the conventional EWMA procedure and allows for dynamically adjusting the weight allocated to the current observation based on the forecast error. In this paper, we extend AEWMA procedures for monitoring linear drifts in process means. An integral equation approach was developed to evaluate the ARL performance

Table 6
Nearly optimal parameters for AEWMA charts under linear drifts when $ARL_0 = 100$, 200, and 250.

θ_1	θ_2	$ARL_0 = 100$			$ARL_0 = 200$			$ARL_0 = 250$		
		λ	γ	c_2	λ	γ	c_2	λ	γ	c_2
0.01	0.05	0.074	3.70	2.039	0.059	3.85	2.281	0.056	4.00	2.361
	0.10		3.70	2.039		3.85	2.281		4.00	2.361
	0.15		3.70	2.039		3.85	2.281		4.00	2.361
	0.20		3.45	2.047		3.50	2.296		3.25	2.414
	0.25		2.90	2.121		3.10	2.357		3.25	2.414
	0.30		2.90	2.121		2.65	2.687		2.95	2.527
	0.50		2.55	2.320		2.65	2.687		2.85	2.620
0.02	0.05	0.100	3.80	2.148	0.083	3.85	2.398	0.079	3.85	2.479
	0.10		3.80	2.148		3.85	2.398		3.85	2.479
	0.15		3.80	2.148		3.85	2.398		3.85	2.479
	0.20		3.30	2.164		3.60	2.406		3.85	2.479
	0.25		3.30	2.164		3.45	2.414		3.50	2.493
	0.30		3.30	2.164		3.10	2.467		3.25	2.525
	0.50		2.55	2.387		2.75	2.631		2.75	2.765
0.03	0.05	0.119	3.90	2.207	0.102	3.90	2.463	0.098	3.95	2.543
	0.10		3.90	2.207		3.90	2.463		3.95	2.543
	0.15		3.90	2.207		3.90	2.463		3.80	2.545
	0.20		3.90	2.207		3.75	2.465		3.80	2.545
	0.25		3.60	2.211		3.75	2.465		3.80	2.545
	0.30		3.15	2.234		3.25	2.498		3.25	2.585
	0.50		2.55	2.422		2.65	2.741		2.90	2.686

Table 7
Nearly optimal parameters for AEWMA charts under linear drifts when $ARL_0 = 300$, 400, and 500.

θ_1	θ_2	$ARL_0 = 300$			$ARL_0 = 400$			$ARL_0 = 500$		
		λ	γ	c_2	λ	γ	c_2	λ	γ	c_2
0.01	0.05	0.054	3.95	2.430	0.051	4.00	2.533	0.049	4.00	2.614
	0.10		3.95	2.430		3.90	2.535		4.00	2.614
	0.15		3.65	2.440		3.90	2.535		3.85	2.617
	0.20		3.40	2.463		3.40	2.576		3.55	2.640
	0.25		3.20	2.502		3.20	2.627		3.15	2.752
	0.30		3.05	2.565		3.20	2.627		3.00	2.867
	0.50		2.90	2.682		2.95	2.785		3.00	2.867
0.02	0.05	0.077	4.00	2.545	0.073	3.95	2.648	0.071	4.00	2.727
	0.10		4.00	2.545		3.95	2.648		4.00	2.727
	0.15		4.00	2.545		3.95	2.648		4.00	2.727
	0.20		3.80	2.549		3.80	2.650		3.80	2.731
	0.25		3.45	2.568		3.45	2.676		3.40	2.766
	0.30		3.25	2.600		3.45	2.676		3.40	2.766
	0.50		2.80	2.813		2.85	2.934		3.00	2.940
0.03	0.05	0.095	4.00	2.607	0.091	4.00	2.709	0.088	4.00	2.785
	0.10		4.00	2.607		4.00	2.709		4.00	2.785
	0.15		3.85	2.609		4.00	2.709		4.00	2.785
	0.20		3.85	2.609		3.75	2.714		3.85	2.788
	0.25		3.55	2.621		3.75	2.714		3.65	2.796
	0.30		3.55	2.621		3.45	2.733		3.35	2.829
	0.50		2.80	2.852		2.90	2.913		3.00	2.957

of AEWMA charts under linear drifts in the mean. This simplifies the analysis of the AEWMA chart without running a large number of simulations.

The comparison results show that the AEWMA chart with varying weights is more powerful than the traditional EWMA. Moreover, it is shown that the AEWMA chart performs closely to the combined Shewhart–EWMA chart when detecting small drifts but achieves a slight advantage in detecting drifts of relatively large coefficients. As compared to the sophisticated control charts such as the GEWMA and GLRT methods, the AEWMA chart is efficient in signaling small drifts but less efficient in signaling large drifts. However, the AEWMA chart has a simpler form than both the GEWMA and GLRT methods. Thus, the AEWMA is quite simple to implement in practice.

This paper mainly focuses on the two-sided AEWMA chart aimed at detecting both positive and negative drifts in the mean. For detecting one-sided positive (or negative) drifts in the mean, the AEWMA chart can be simply modified by only removing the lower (or upper) control limit. The above integral equation can be similarly employed to analyze the ARL performance of a one-sided AEWMA chart. Given the same design parameters (λ, γ, and c_2), the in-control ARL of the one-sided AEWMA chart would be twice that of the two-sided AEWMA chart. Furthermore, parallel to the issue of monitoring

Table 8
Nearly optimal parameters for AEWMA charts under linear drifts when $ARL_0 = 600$, 800, and 1000.

θ_1	θ_2	$ARL_0 = 600$			$ARL_0 = 800$			$ARL_0 = 1000$		
		λ	γ	c_2	λ	γ	c_2	λ	γ	c_2
0.01	0.05	0.047	4.00	2.6748	0.045	4.00	2.776	0.043	4.00	2.849
	0.10		3.95	2.6758		3.90	2.779		4.00	2.849
	0.15		3.95	2.6758		3.90	2.779		3.85	2.855
	0.20		3.45	2.7207		3.65	2.800		3.55	2.891
	0.25		3.25	2.7825		3.40	2.849		3.55	2.891
	0.30		3.25	2.7825		3.10	3.035		3.25	3.015
	0.50		3.10	2.8872		3.10	3.035		3.20	3.090
0.02	0.05	0.069	3.95	2.7896	0.066	4.00	2.884	0.065	4.00	2.962
	0.10		3.95	2.7896		4.00	2.884		4.00	2.962
	0.15		3.95	2.7896		4.00	2.884		4.00	2.962
	0.20		3.65	2.8027		4.00	2.884		4.00	2.962
	0.25		3.45	2.8267		3.55	2.913		3.55	2.999
	0.30		3.20	2.8887		3.35	2.955		3.55	2.999
	0.50		3.00	3.0469		3.10	3.103		3.15	3.178
0.03	0.05	0.086	4.00	2.8477	0.083	4.00	2.943	0.081	4.00	3.016
	0.10		4.00	2.8477		4.00	2.943		4.00	3.016
	0.15		4.00	2.8477		4.00	2.943		4.00	3.016
	0.20		3.90	2.8491		4.00	2.943		4.00	3.016
	0.25		3.70	2.8569		3.90	2.946		3.80	3.023
	0.30		3.45	2.8801		3.35	3.003		3.45	3.064
	0.50		2.95	3.0984		3.05	3.152		3.10	3.238

linear drifts in the mean, monitoring linear drifts in process variances is equally important. The proposed technique can be employed for this purpose. This research work will be pursued in the future.

Acknowledgments

We are grateful to the Editor and two anonymous referees for their insightful suggestions that significantly improved the quality of this paper. Yan Su's work was supported in part by the Start-Up Research Grant (SRG) SRG009-FST11-YS. Lianjie Shu's work was supported in part the Research Committee under the grant RG011/09-10S. Kwok-Leung Tsui's research was supported in part by RGC/GRF Grant 9041578.

References

Baker, C.T.H., 1977. The Numerical Treatment of Integral Equations. Clarendon Press, Oxford, England.
Bissell, A.F., 1984. The performance of control charts and CUSUMs under linear trend. Appl. Stat. 33, 145–151.
Brook, D., Evans, D.A., 1972. An approach to the probability distribution of CUSUM run length. Biometrika 59, 539–549.
Capizzi, G., Masarotto, G., 2003. An adaptive exponentially weighted moving average control chart. Technometrics 45, 199–207.
Davis, R.B., Krehbiel, T.C., 2002. Shewhart and zone control chart performance under linear trend. Comm. Statist. Simulation Comput. 31, 91–96.
Davis, R.B., Woodall, W.H., 1988. Performance of the control chart trend rule under linear shift. J. Qual. Technol. 20, 260–262.
Domangue, R., Patch, S.C., 1991. Some omnibus exponentially weighted moving average statistical process monitoring schemes. Technometrics 33, 299–313.
Fahmy, H.M., Elsayed, E.A., 2006a. Detection of linear trends in process mean. Int. J. Prod. Res. 44, 487–504.
Fahmy, H.M., Elsayed, E.A., 2006b. Drift time detection and adjustment procedures for processes subject to linear trend. Int. J. Prod. Res. 44, 3257–3278.
Gan, F.F., 1991. EWMA control chart under linear drift. J. Stat. Comput. Simul. 38, 181–200.
Gan, F.F., 1992. CUSUM control charts under linear drift. Statistician 41, 71–84.
Gan, F.F., 1996. Average run lengths for cumulative sum control charts under linear trend. Appl. Stat. 45, 505–526.
Hackbusch, W., 1995. Integral Equations: Theory and Numerical Treatment. In: International Series of Numerical Mathematics, vol. 120. Birkhäuser, Basel, Boston, Berlin.
Han, D., Tsung, F., 2004. A generalized EWMA control chart and its comparison with the optimal EWMA, CUSUM and GLR schemes. Ann. Stat. 32, 316–339.
Holland, P.W., Welsch, R.E., 1977. Robust regression using iteratively reweighted least-squares. Comm. Statist. Theory Methods 6, 813–827.
Huber, P.J., 1981. Robust Statistics. John Wiley & Sons, New York, NY.
Koning, A.J., Does, R.J., 2000. CUSUM charts for preliminary analysis of individual observations. J. Qual. Technol. 32, 122–132.
Lucas, J.M., Crosier, R.B., 1982. Fast initial response for CUSUM quality control schemes: give your CUSUM a head start. Technometrics 24, 199–205.
Lucas, J.M., Saccucci, M.S., 1990. Exponentially weighted moving average control schemes: properties and enhancements. Technometrics 32, 1–12.
Mahmoud, M.A., Zahran, A.R., 2010. A multivariate adaptive exponentially weighted moving average control chart. Comm. Statist. Theory Methods 39, 606–625.
Montgomery, D.C., 2009. Introduction to Statistical Quality Control, 7th ed. John Wiley & Sons, New York.
Rainer, G., Castillo, E.D., Ratz, M., 2001. Run length comparisons of Shewhart charts and most powerful test charts for the detection of trends and shifts. Comm. Statist. Simulation Comput. 30, 355–376.
Reynolds, M.R., Stoumbos, Z.G., 2001. Individuals control schemes for monitoring the mean and variance of processes subject to drifts. Stoch. Anal. Appl. 19, 863–892.
Runger, G.C., Testik, M.C., 2003. Control charts for monitoring fault signatures: Cuscore versus GLR. Qual. Reliab. Eng. Int. 19, 387–396.
Shu, L., 2008. An adaptive exponentially weighted moving average control chart for monitoring process variances. J. Stat. Comput. Simul. 78, 367–384.
Shu, L., Jiang, W., Wu, Z., 2008. Adaptive CUSUM procedures with Markovian mean estimation. Comput. Statist. Data Anal. 52, 4395–4409.
Simões, B.F.T., Epprecht, E.K., Costa, A.F.B., 2010. Performance comparisons of EWMA control chart schemes. Qual. Technol. Quant. Manag. 7, 249–261.
Tseng, S.T., Jou, B.Y., Liao, C.H., 2010. Adaptive variable EWMA controller for drifted processes. IIE Trans. 42, 247–259.
Tseng, S.T., Tsung, F., Liu, P.Y., 2007. Variable EWMA run-to-run controller for drifted processes. IIE Trans. 39, 291–301.
Woodall, W.H., Mahmoud, M.A., 2005. The inertial properties of quality control charts. Technometrics 47, 425–436.
Yashchin, E., 1995. Estimating the current mean of a process subject to abrupt changes. Technometrics 37, 311–323.
Zou, C., Liu, Y., Wang, Z., 2009. Comparisons of control schemes for monitoring the mean of processes subject to drifts. Metrika 70, 141–163.